Stability of Rocksalt (111) Polar Surfaces: Beyond the Octopole

Fabio Finocchi,[1] Antoine Barbier,[2] Jacques Jupille,[1] and Claudine Noguera[1]
[1]*Groupe de Physique des Solides, UMR 7588 CNRS and Universités Paris 6 - Paris 7, Campus de Boucicaut, 140 rue de Lourmel, 75015 Paris, France*
[2]*CEA/Saclay, DRECAM-SPCSI, 91191 Gif-Sur-Yvette, France*

(Received 8 July 2003; published 30 March 2004)

Stable polar oxide surfaces must be simultaneously electrostatically compensated and in thermodynamic equilibrium with the environment. As a paradigm, the MgO(111)-$p(2 \times 2)$ reconstructed surface is shown to involve combinations of Mg-covered terminations with peculiar insulating electronic structure, favored in O-poor conditions, and the O-terminated octopole, stabler in more O-rich environments. Such a picture, which could not have been foreseen by either experiments or simulations separately, goes beyond the Wolf model and reconciles the theory with the experimental data taken in variable thermodynamic conditions.

DOI: 10.1103/PhysRevLett.92.136101 PACS numbers: 68.35.Bs, 61.10.Nz, 68.35.Dv, 68.47.Gh

Understanding the stability of metal oxide (MO) surfaces is an issue encompassing a wide class of problems in geology [1], environmental sciences, microelectronics, catalysis, and fundamental physics [2]. MO surfaces are indeed very sensitive to the ambient conditions. In particular, they often undergo profound and not yet well understood changes in atomic-scale morphology and stoichiometry at much lower temperatures than those characteristic of atomic self-diffusion.

In this respect, the *polar* MO surfaces deserve increasing attention. Polar orientations occur whenever a ionocovalent crystal is cut normally to directions along which the bulk unit cell carries a net dipole moment [3], which implies a divergence of the electrostatic potential. Their thermodynamic stability requires major rearrangements, which can be driven by changes in surface composition or anomalous filling of surface states [4]. Indeed, recent results point to a subtle competition between distinct surface configurations and a special sensitivity to the chemical environment. The morphology and stoichiometry of various reconstructions of $Al_2O_3(0001)$ [5,6], and of the (0001) orientation of α-Fe_2O_3 [7] and ZnO [8,9], were found to be much affected by the external conditions and, for some phases, to show peculiar electronic properties. Stabilization by nonstoichiometric reconstructions, metallization through thermal decomposition, or even sublimation in oxygen poor conditions of the (111) terminations of rocksalt MO crystals NiO [10–13], MgO [14,15], CoO, and MnO [16] suggests the coexistence of several motifs depending on the temperature, oxygen potential, and elaboration mode.

However, the rationale for the existence of several phases for a polar MO termination as a function of the actual thermodynamic conditions has not been elucidated yet, although it is a key ingredient of the stability of these surfaces in environments as diverse as ultrahigh vacuum (UHV) or normal atmospheric pressure, not to mention strong changes in temperature. The case of the alkali-metal oxide MgO is especially interesting, since no competing bulk phases exist at normal conditions, as it happens for some transition MO having cations with multiple oxidation states. Neglecting the chemical environment, the $p(2 \times 2)$ octopole reconstruction [17] was predicted for the prototypical MgO(111) polar surface. It consists of either Mg or O terminations with "Mg_1-O_3-Mg_4" (Mg-oct) or "O_1-Mg_3-O_4" (O-oct) stoichiometries, respectively, according to the number of atoms per unit cell in the three outermost layers going from the surface into the bulk. Although the octopole reconstruction fulfills the polarity compensation, it appears to be unable to explain the outcome of many recent experiments on the (111) terminations of rocksalt MO [12,14,16]. In the following, we show that it is mandatory to combine experiments and theory to solve this issue and provide a coherent picture of the $p(2 \times 2)$ reconstructions of MgO(111) as a function of the thermodynamic conditions.

The experimental data on MgO(111) were obtained through grazing incidence x-ray diffraction (GIXD) measurements performed on the ID03 beam line at European Synchrotron Radiation Facility (ESRF) [18] in UHV. A dozen independent data sets were collected in the temperature range $100 \leq T \leq 520$ K under variable oxygen partial pressure P_{O_2}. The upper T limit at low P_{O_2} was chosen to avoid irreversible structural decomposition of the surface [15]. The MgO(111) crystals were first annealed at 1850 K in air to provide high quality shining, flat, and well crystallized surfaces. A mosaic spread as small as 14 mrad and a large domain size enabled accurate GIXD quantitative measurements, the best conditions being achieved for an incidence angle corresponding to the total external reflection (0.13° at 17.1 keV). The measured intensities were corrected for background, active area and Lorentz, monitor, and polarization factors [19,20]. In most cases, all accessible positions belonging to the in-plane pattern, which showed a $P6mm$ symmetry with a systematic error level below 10%, were analyzed by

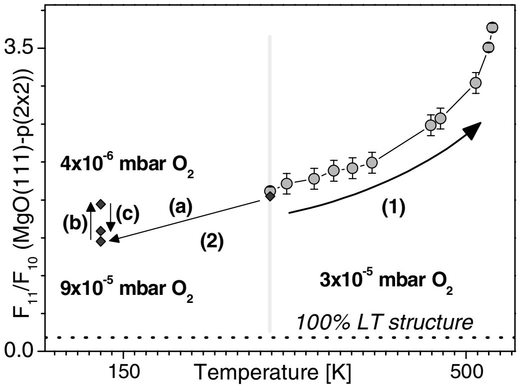

FIG. 1. Ratio between the in surface plane (11) and (10) $p(2 \times 2)$ reconstruction structure factors as a function of temperature T and oxygen partial pressure P_{O_2}. (1) T increases and $P_{O_2} = 3 \times 10^{-5}$ mbar. (2a) T decreases and $P_{O_2} = 9 \times 10^{-5}$ mbar. At low T, P_{O_2} is first decreased (2b) to $4 \times 10 - 6$ mbar and then increased again (2c) to 9×10^{-5} mbar. The horizontal dotted line indicates the expected ratio for the LT pure structure, while a ratio of 11.6 corresponds to the HT structure (see text). The LT and HT experiments were performed on two different samples.

rocking scans. Out of plane measurements along diffraction and crystal truncation rods were also performed. The striking observation is that the Patterson diagram (PD) shows dramatic and partially reversible evolutions upon changes in P_{O_2} and T, even below the ambient temperature. Especially noteworthy are the large variations in the relative intensities of the two (11) and (10) reconstruction peaks closest to the direct beam. Their factor structure ratio appears as a very convenient tool to monitor the changes in surface structure (Fig. 1). Although the $p(2 \times 2)$ periodicity is always observed, these data unambiguously demonstrate the occurrence of at least two distinct motifs, herein labeled HT and LT (high/low temperature), the LT/HT transition being clearly driven by the temperature and the oxygen chemical potential.

To interpret the PD changes on the basis of a microscopic model, *ab initio* simulations were carried out, by using the density functional theory (DFT) and pseudopotential plane-wave techniques [21]. Up to nine special k points were used in the irreducible Brillouin zone. The various $p(2 \times 2)$ surfaces were modeled by slabs for which any laterally averaged quantity is symmetric under inversion, and thick enough to reduce the uncertainty on the computed surface energies to 0.1 J/m^2. The residual atomic forces after geometry optimization are below 10 meV/Å.

The model involving the theoretically predicted Mg-oct and O-oct (Fig. 2, left) reconstructions [17] fails in fitting the HT GIXD data. Bearing in mind the proposed motifs for NiO(111)-$p(2 \times 2)$ [12], it was then assumed that the Mg-oct might coexist with the so-called O-terminated spinel (O-spi) having the same "O_1-Mg_3-O_4" stoichiometry as the O-oct. In the O-oct, the outermost O atom is bonded to three equivalent subsurface Mg. In the O-spi, it is atop one of the subsurface Mg, which are notably inequivalent, an essential ingredient to account for the outcome of GIXD. Though the (Mg-oct, O-spi) model nicely fits the experimental data, the existence of the O-spi is questioned by the calculations. Consistently with the presence of the onefold coordinated surface oxygen, the O-spi has a much higher surface energy (4.5 J/m^2) than the O-oct (2.1 J/m^2). Its instability versus the O-oct against any small atomic displacement definitely discards the model.

Up to that point, the composition of the surface layers was chosen according to schemes involving Mg and O ions with formal charges of equal absolute values, which restricts the stoichiometry of compensated surfaces to "O_n-Mg_l-O_m" or "Mg_n-O_l-Mg_m," with $n - l + m = \pm 2$. Yet, the undisputable experimental finding that at least two motifs coexist on the MgO(111) surface as a function of P_{O_2} and T (Fig. 1), as well as the failure of all above mentioned attempts prompted us to scrutinize the

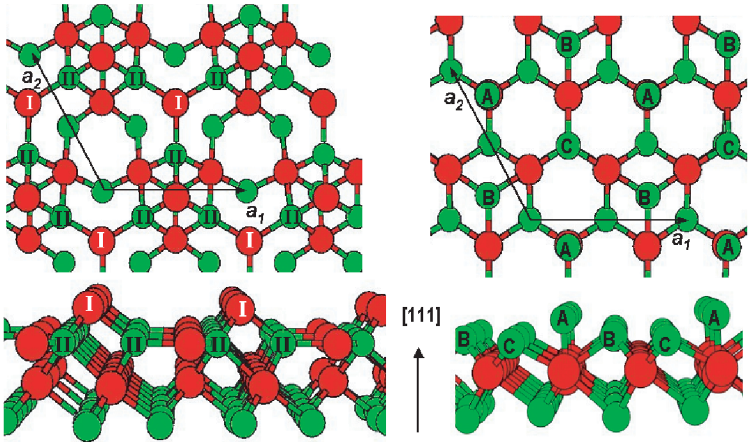

FIG. 2 (color online). Top and side views of the O-oct (left) and the α-Mg/OMg (right) $p(2 \times 2)$ optimized configurations. Mg are gray and O atoms are dark gray. In the O-oct model, "I" and "II" indicate the outermost layer and that beneath, respectively. In the α-Mg/OMg configuration, the inequivalent surface Mg are labeled A, B, and C.

chemical content of the surface layers. The analogy with NiO(111), on which metallic clusters were found for very O-poor conditions [12], suggests that surface cations can show distinct charge states when MgO(111) is exposed to reducing conditions. The existence of nonequivalent cations as shown from the low P_{O_2} PD's supports this picture. To explore such a scheme, Mg-covered MgO(111) configurations, corresponding to a "Mg_3-O_4" stoichiometry—the simplest one giving rise to metal-rich surfaces, yet never considered previously—were simulated. Configurations of different stoichiometry, including other $p(2 \times 2)$ reconstructions such as the ozonelike one [14] were discarded, since they show too high surface energies and badly account for the GIXD data [22].

The most favorable arrangement consisted in a (0001)-oriented epitaxial Mg layer on the O-terminated MgO(111), hereafter noted as α-Mg/OMg, and sketched in Fig. 2, right. Although α-Mg/OMg corresponds to a "Mg_3-O_4" stoichiometry that does not automatically ensure the polarity compensation, it is insulating and compensated simultaneously, with a DFT highest occupied molecular orbital–lowest unoccupied molecular orbital (HOMO-LUMO) gap comparable to the O-oct. In α-Mg/OMg the polarity is compensated through an anomalous filling of a surface state, as confirmed by the analysis of the computed topological atomic charges [23]. At variance with the case of neutral metal adlayers on MgO(111) [24], the two 3-fold coordinated surface $Mg^{(3)}$ are ionized, while the 1-fold coordinated $Mg^{(1)}$ (labeled A in Fig. 2) is almost neutral. The HOMO is mostly localized around $Mg^{(1)}$. Its level lies in the gap of bulk MgO, well below the conduction band, consistently with the weak Madelung potential exerted on $Mg^{(1)}$ by the neighboring charges. Such a peculiar electronic structure is partly responsible for the very low computed surface stress of α-Mg/OMg, despite the large nominal mismatch of a Mg(0001) layer on MgO(111). α-Mg/OMg is a very uncommon case of a nonstoichiometric configuration that has an anomalous filling and is insulating. Although each of these characteristics can happen for a particular surface reconstruction [7–9,13], they were never encountered at the same time.

To complete the picture of the $p(2 \times 2)$ reconstruction of MgO(111) by accounting for both diffraction data and stability criteria determined by first-principles calculations, a mixing of distinct surface configurations was necessary. Aiming at a full consistency between the experimental data and the theoretical models, we have evaluated the GIXD structure factors [25] starting from the simulated motifs, by using the computed atomic charges [23] and positions. The only adjustable parameter was the weight of each configuration. Out of those tests, only a combination of O-oct and α-Mg/OMg configurations (Fig. 2) remained as an acceptable candidate. According to the best fit, partially shown in Fig. 3, the surface composition evolves considerably as a function of the temperature. At $T = 100$ K, a structure with an equal proportion of O-oct and α-Mg/OMg perfectly fits the GIXD data [26]. At $P_{O_2} = 3 \times 10^{-5}$ mbar, the fraction of α-Mg/OMg increases with T, raising up to 72% at $T = 300$ K and to 87% at $T = 520$ K. At odds with the current opinion that the $p(2 \times 2)$ reconstruction of MgO(111) can be simply explained by the octopole, the present model reveals the complexity of the surface structure that cannot in any case be accounted for by a unique geometry.

The crucial issue of the surface stability with respect to the external conditions was examined by calculating the surface grand potential per unit area γ_s at $T = 0$ K, as a function of the excess O chemical potential $\Delta\mu_O$ [27], which is a critical parameter for most oxide surfaces [7,9]. For α-Mg/OMg, γ_s linearly decreases as a function of $\Delta\mu_O$, from 5.0 J/m^2 ($\Delta\mu_O = 0$) to 1.9 J/m^2 at the lower limit ($\Delta\mu_O = -6.1$ eV). α-Mg/OMg becomes slightly more stable than the O-oct in O-poor environments (see Fig. 4). Therefore, the emergence of the α-Mg/OMg in

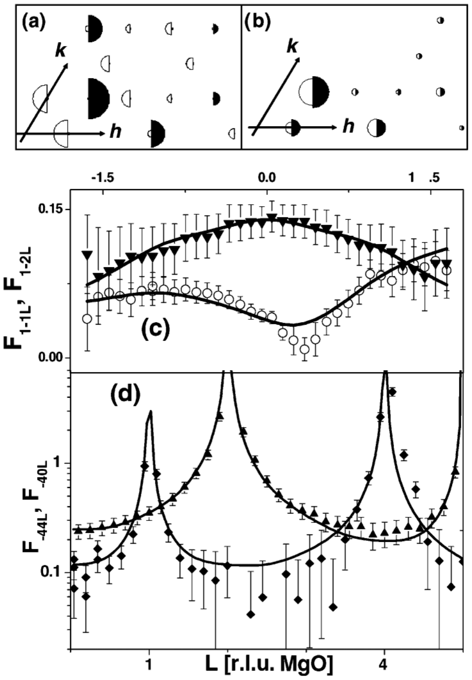

FIG. 3. MgO(111)-$p(2 \times 2)$ reconstruction structure factors (SF). (a) SF computed for the pure DF optimized geometries. Left half circles: the *LT* [O-oct, Fig. 2, left] SF. Right half circles: the *HT* [α-Mg/OMg, Fig. 2, right] SF. (b) White half circles: Measured (room *T*) in surface plane reconstruction peak SF, compared to the calculated SF from a combination of 28% O-oct and 72% α-Mg/OMg (black half circles), with a Debye-Waller factor of 4 Å^2. (c) ($1\bar{1}$L) (○) and ($1\bar{2}$L) (▼) diffraction rods SF measured at $T = 520$ K compared with the theoretical SF derived from the 13% O-oct + 87% α-Mg/OMg model (straight lines). A Debye-Waller factor of 18 Å^2 was fitted and the χ^2 was 0.56 for the corresponding in surface plane data. (d) Experimental ($\bar{4}$4L) (△) and ($\bar{4}$0L) (◆) and computed (straight lines) crystal truncation rods obtained in the same conditions as described in (c). *L* describes the perpendicular momentum transfer in units of the $p(2 \times 2)$ reciprocal *h* and *k* lattice vectors.

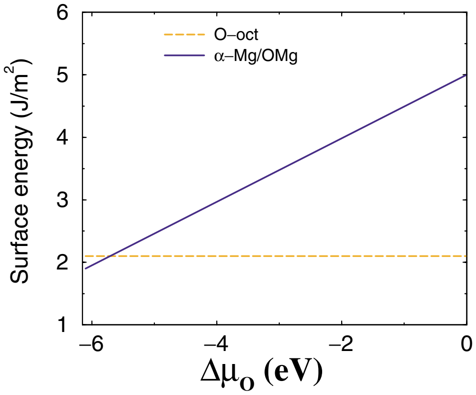

FIG. 4 (color online). Computed surface energy γ_s of the O-oct and α-Mg/OMg configurations of MgO(111) $p(2 \times 2)$, as a function of the excess oxygen chemical potential $\Delta\mu_{\mathrm{O}}$.

the *HT* phase is supported by data fitting and, independently, by the surface energy. Finally, the proposed transition from O-oct ("O_1-Mg_3-O_4") to the α-Mg/OMg ("Mg_3-O_4") configurations (and vice versa) is chemically consistent, since it involves the removal of the apex O in the O-oct according to the actual redox conditions as well as local relaxations, without any interlayer atomic diffusion. As a first approximation, this can be mapped onto an Ising model: the two surface motifs with or without the apex oxygen correspond to $s = 1$ or $s = -1$ states, respectively, and the increase of O chemical potential acts as a magnetic field on the Ising spin assembly [22]. Because of the presence of soft vibrations involving $Mg^{(1)}$ in α-Mg/OMg, finite temperature effects on the $T = 0$ K phase diagram (Fig. 4) should stabilize the latter configuration over O-oct slightly, thus widening the stability region of α-Mg/OMg in terms of $\Delta\mu_{\mathrm{O}}$ [22].

The present study provides a key to interpret the evolution of the (111) faces of other rocksalt metal oxides in terms of a comprehensive structural model. For instance, the interpretation of the NiO(111) $p(2 \times 2)$ reconstruction [12] should probably be reconsidered in the light of the above discussion, yet requiring a careful treatment of the exchange and correlation effects [28,29] beyond the present approach [30]. With respect to thermodynamic conditions, all MO(111) $p(2 \times 2)$ reconstructions show a competition between distinct structures, of which the celebrated octopole model is just one particular realization in quite O-rich environments. In very reducing conditions, and as a function of temperature, metal-rich surfaces are more stable and can keep on being insulating.

More generally, the strategy devised here can be useful to disentangle the structure of other (polar) oxide surfaces that are characterized by a competition between various configurations and take benefit from their sensitivity to the external conditions to design surfaces with specific reactivity. For instance, flat and stoichiometric MgO(100) is almost inert, while MgO(111) $p(2 \times 2)$ can display a varying activity as a function of the ambient conditions. Because of its peculiar surface electronic structure with an almost neutral Mg, the α-Mg/OMg configuration can be predicted to be more active than the O-terminated octopole. Metals should strongly adhere on the Mg outermost layer, as found in the case of magnetic alloys on the NiO(111) single crystal surface [31]. The tunable reactivity of MgO(111) should also affect the adsorption and dissociation of molecular species, with potential applications in catalysis and gas sensing.

Most calculations were performed at the IDRIS-CNRS computer center. We thank Christiane Caroli and Jacek Goniakowski for critical comments, Christian Mocuta for participating in an early experiment, and the ID03 beam line staff for technical support.

[1] W. H Casey and C. Ludwig, Nature (London) **381**, 506 (1996).
[2] See, e.g., J. Jupille, Surf. Rev. Lett. **8**, 69 (2001).
[3] P.W. Tasker, J. Phys. C **12**, 4977 (1979).
[4] C. Noguera, J. Phys. Condens. Matter **12**, R367 (2000).
[5] G. Renaud, Surf. Sci. Rep. **32**, 5 (1998).
[6] X. G. Wang, A. Chaka, and M. Scheffler, Phys. Rev. Lett. **84**, 3650 (2000).
[7] X. G. Wang *et al.*, Phys. Rev. Lett. **81**, 1038 (1998).
[8] A. Wander *et al.*, Phys. Rev. Lett. **86**, 3811 (2001).
[9] O. Dulub, U. Diebold, and G. Kresse, Phys. Rev. Lett. **90**, 016102 (2003).
[10] C. A. Ventrice *et al.*, Phys. Rev. B **49**, 5773 (1994).
[11] F. Rohr *et al.*, Surf. Sci. **315**, L977 (1994).
[12] A. Barbier *et al.*, Phys. Rev. Lett. **84**, 2897 (2000).
[13] N. Erdman *et al.*, Surf. Sci. **470**, 1 (2000).
[14] R. Plass *et al.*, Phys. Rev. Lett. **81**, 4891 (1998).
[15] V. E. Heinrich, Surf. Sci. **57**, 385 (1976).
[16] G. Renaud and A. Barbier, in *The Chemical Physics of Solid Surfaces* (Elsevier, New York, 2001), Vol. 9, p. 256.
[17] D. Wolf, Phys. Rev. Lett. **68**, 3315 (1992).
[18] http://www.esrf.fr.
[19] E. Vlieg, J. Appl. Crystallogr. **30**, 532 (1997).
[20] O. Robach *et al.*, J. Appl. Crystallogr. **33**, 1006 (2000).
[21] X. Gonze *et al.*, Comput. Mater. Sci. **25**, 478 (2002).
[22] A longer report will be given in a forthcoming paper.
[23] R. F.W. Bader, Chem. Rev. **91**, 893 (1991).
[24] J. Goniakowski and C. Noguera, Phys. Rev. B **66**, 085417 (2002).
[25] The data were worked out with the ROD software available at www.esrf.fr.
[26] In α-Mg/OMg, the main contribution to the structure factors comes from the array of surface Mg, which closely resembles that found at the O-spi.
[27] The excess O chemical potential $\Delta\mu_{\mathrm{O}} = \mu_{\mathrm{O}} - \mu_{\mathrm{O_2(gas)}}$ is negative and bounded from below by the formation energy of $MgO_{(c)}$ with respect to $O_{2(gas)}$ and $Mg_{(c)}$.
[28] A. Svane and O. Gunnarsson, Phys. Rev. Lett. **65**, 1148 (1990).
[29] D. Ködderitzsch *et al.*, Phys. Rev. B **66**, 064434 (2002).
[30] J. P. Perdew, R. Burke, and M. Enzerhof, Phys. Rev. Lett. **77**, 3865 (1996).
[31] C. Mocuta *et al.*, Phys. Rev. B **68**, 014416 (2003).